2019 IEEE International Conference on Systems, Man and Cybernetics (SMC)
Bari, Italy, October 6-9, 2019

Detection and evaluation of events in EEG dynamics in post-surgery patients with physiological-based mathematical models*

Eva Dulf[1], Maria Ghita[2,3] and Clara M. Ionescu [1,2,3]

***Abstract*— As part of the new directions for vision and mission of Europe, patient well-being and healthcare become core features of a modern and prosperous society. That is, healthcare costs are optimized towards patient benefit and sideways effects such as cost-related reduction in medication, in frequency of post-operatory interventions, in recovery times and in comorbidity risk. In this paper, we address the incidence of events related to stroke, epileptic seizures and tools to possibly predict their presence from Electroencephalography (EEG) signal acquired in post-surgery patients. Wavelet analysis and spectrogram indicate graphically changes in the energy content of the EEG signal. Physiologically based neuronal dynamic pathway is used to derive fractional order impedance models. Nonlinear least squares identification technique is used to identify model parameters, with results suggesting parameter redundancy. There is a significant difference in model parameter values between EEG signal with/-out events.**

I. INTRODUCTION

Patient well-being and healthcare can be best described as bringing longer life and an improved quality of life for patients. The value of the treatment is determined by the amount of clinical benefit it can achieve balanced against its cost, beside its effects. Next to chronic pain and rehabilitation management, epilepsy, stroke and aneurysm are significant phenomena with long tails in the socio-economic impact on total costs for healthcare.

A brain aneurysm is a bulge in an artery in the brain that has the potential to burst or rupture. A ruptured aneurysm can cause a type of stroke called a subarachnoid hemorrhage. An estimated 3% of United States of America population may have or develop a brain aneurysm each year, according to the Mayfield Clinic [1]. Not all aneurysms cause stroke, and vice-versa. However, if a person is at risk for a burst aneurysm, treatment is often required to prevent this potentially life-threatening occurrence. Medical specialists do not pre-detect an estimated 85% of aneurysms (only after they burst). A stroke may occur due to either the blood supply to the brain being blocked or a blood vessel in the brain rupturing. Two stroke types exists: hemorrhagic and ischemic. Hemorrhagic strokes are usually the result of one of two causes: an aneurysm or a collection of abnormal blood vessels in the brain that can rupture. Ischemic strokes are those that result from a blockage in an artery in the brain. When a blood clot breaks free from its place in an artery, it can lodge in a portion of the brain. This keeps blood from flowing freely to the brain. Without the oxygen and nutrients that the blood brings to the brain tissue, the tissue dies. The result can be impaired body functioning or death, while some of impairment is indirectly related to other dysfunctions such as multiple sclerosis, semi-paralysis, speech/mobility impairment etc.

In practice, the decision of whether to treat incidental intracranial saccular aneurysms is complicated by limitations in current knowledge of their natural history. A systematic review and pooled analysis of individual patient data from 8.382 participants in six prospective cohort studies with subarachnoid haemorrhage as outcome was reported in [2]. Rupture occurred in 230 patients during 29.166 person-years of follow-up. The mean observed 1-year risk of aneurysm rupture was 1.4% (with 95% confidence interval $1.1-1.6$) and the 5-year risk was 3.4% (with 95% confidence interval $2.9-4.0$). Prediction factors were age, hypertension, history of subarachnoid haemorrhage, aneurysm size, aneurysm location, and geographical region. In study populations from North America and European countries other than Finland, the estimated 5-year absolute risk of aneurysm rupture ranged from 0.25% in individuals younger than 70 years without vascular risk factors with a small-sized ($<$ 7 mm) internal carotid artery aneurysm, to more than 15% in patients aged 70 years or older with hypertension, a history of subarachnoid haemorrhage, and a giant-sized ($>$ 20 mm) posterior circulation aneurysm. By comparison with populations from North America and European countries other than Finland, Finnish people had a 3.6-times increased risk of aneurysm rupture and Japanese people a 2.8-times increased risk.

SAFE (Stroke Alliance For Europe) commissioned the Burden of Stroke study to show each EU country where it stands compared to others in terms of the stroke burden and how well it is meeting the need for acute and follow-up care, including examples of good practice (https://strokeeurope.eu/).

The Burden of Stroke in Europe research shows in 2017 shocking disparities between and within countries along the entire stroke care pathway. Europe-wide comparisons of stroke and stroke care are vital to help each country prevent stroke and provide better care and support for everyone affected by it. To make accurate comparisons between different

*This work has been supported by Special Research Fund of Ghent University BOFSTG-2018, MIMOPREC project, and Flanders Research Center grant nr. 3SO4719.

[1]Technical University of Cluj-Napoca, Department of Automation, Memorandumului street, no.28, Cluj Napoca, Romania. eva.dulf@aut.utcluj.ro

[2]Dynamical Systems and Control research group, Ghent University, Tech Lane Science Park 125, 9052 Ghent, Belgium. maria.ghita@UGent.be, claramihaela.ionescu@UGent.be

[2]EEDT core lab on decision and control, Flanders Make consortium, Tech Lane Science Park 131, 9052 Ghent, Belgium.

countries, populations and health systems, we need coordinated Europe-wide data collection. Therefore, European policy-makers, in particular the European Commission and the Joint Research Centre, should support and promote the use of a robust Europe-wide stroke register to assess quality of care along the whole stroke pathway.

In Romania, the majority of population is covered through contributions to social insurance system; free at point of use for all [3]. For stroke epidemiology, on the population of 19.043.767, the incidence estimate (Global Burden of Disease - GBD 2015) is 61.552 strokes/year, 191 strokes per 100.000 inhabitants annually, the prevalence estimate (GBD 2015) is 252.774 strokes, 833 per 100.000 inhabitants and mortality (GBD 2015) is 54.272 deaths due to stroke/year, 156 deaths per 100.000 inhabitants annually, all numbers age- and sex-adjusted [4]. The information is based on registries from Targu Mures Registry (local, only hospitalized patients) [5] and the healthcare cost of stroke: total 163.1 million EUR, i.e. 8 EUR per capita [6].

In Belgium, for a total population of 11.007.020, we have an incidence estimate of (GBD 2015): 10.397 strokes/year, 50 strokes per 100.000 inhabitants annually, a prevalence estimate of (GBD 2015): 63.535 strokes, 348 per 100.000 inhabitants age- and sex-adjusted [4]. The case fatality of ischemic stroke is: 9.2 per 100 discharges, adults aged 45 or older, age- and sex-adjusted, and a mortality rate of 9.501 deaths due to stroke/year, 38.7 deaths per 100.000 inhabitants annually age- and sex-adjusted [7]. The information is based on mandatory hospitalization data, Belgian Sentinel Network of General Practitioners, Institute of Health population surveys and the healthcare cost of stroke in Belgium: total 393.7 million EUR, i.e. 35 EUR per capita [6].

Several major risk factors of aneurysm growth and rupture have been identified. There exist recommendations on diagnostic work up, monitoring and general management (blood pressure, blood glucose, temperature, thromboprophylaxis, anti-epileptic treatment, use of steroids). Apart from the above, leading risks for ischemic stroke are i) hypertension and ii) surgery and anesthesia [8].

In today's EU vision and mission for health and well-being, an important role is played by decision support systems. It has been long acknowledged that medicine and engineering must go hand-in-hand for better results [9]. There is evidence to maintain the claim that decision support systems related to computer based (and implicitly mathematical patient model based) systems for titrating drugs during anesthesia have positive effect on reducing post-surgery secondary effects (time to recovery, post-surgery depression, etc.) [10]. One of the most debilitating complications in the perioperative period with serious clinical sequelae is cerebral ischemia [11].

In this paper, we propose a first hand solution and preliminary results for detecting 'out of the ordinary' events in the EEG signal which may indicate a prevalence for stroke in post-surgery anesthetized patients. The paper is organized as follows. The next section provides background information on the set of data used in this work. Third section gives a summary of the methods used to extract information from the signals followed by a section on results and discussion on further use of the tools proposed. A conclusion section summarizes the main outcome of this work and points to further steps.

II. ON EEG SIGNAL

The study protocol was approved by the local Ethics Committee of Ghent University Hospital (Belgium), and was performed in accordance with the Declaration of Helsinki and the Good Clinical Practice Guideline of the European Commission. Patients were routinely regarded eligible for inclusion according to the following criteria:

- patients in the immediate post-operative phase after a coronary artery bypass graft (CABG) surgery,
- age ≥ 18 years,
- informed consent obtained before the surgery.

Exclusion criteria were patients with:

- renal failure defined by the RIFLE Classification levels: Risk, Failure and End-stage Kidney Failure,
- hepatic failure defined by a bilirubin level of ≥ 3 mg/dl and/or a prothrombin level of $< 50\%$ before the surgery,
- low ejection fraction defined as $< 40\%$,
- age < 18 years,
- postoperative bleeding necessitating surgical revision,
- history of cerebrovascular accident (CVA),
- history of chronic obstructive pulmonary disease (COPD),
- age > 75 years,
- postoperative cardiac index < 2.2 for more than 2 hours,
- mixed venous oxygen saturation (SvO2) $< 60\%$ for more than 2 hours,
- hypo-tension with a mean arterial pressure < 60 mmHg for more than 2 hours.

The EEG signal was acquired in Ghent University Hospital in post-surgery patients during intensive care recovery unit. The EEG signal is recorded from 4 channels located on the front and occipital area of the patient's brain and processed in epochs of overlapping 15 seconds interval windows. When signal quality index is below a threshold of 30%, the window is discarded and the value from previous instant interval is used. In this way, possible delays are introduced in the signal via the processing algorithm. Further on, the signal is calibrated to a scale from 0 (no activity) to 100 (activity). The measurement part of the process involves solely standard equipment.

III. PROPOSED METHODOLOGY

It is possible to characterize a signal in time or frequency domain. However none of these two can cover the main features of the signal completely. Some characteristics are better shown in frequency domain while the other features may be determined more effectively in time domain [12]. In other word, we may not be able to capture some important information in time domain; while, they are clearly apparent in frequency domain and vice versa. Time-Frequency

analysis is one of the approaches that gives a wider view towards the signal, because it has the advantages of both time- and frequency- analysis. A useful approach to evaluate a signal by Time-Frequency analysis is to make use of spectrograms, wavelet analysis, short time Fourier transform etc. According to Fourier theorem, it is assumed that the signal $y = (y_0, y_1, ...y_{N-1})$, with N the number of samples in the signal, is defined by a sum of sinusoids. The aim of a time-frequency transform generally is to discover which sinusoid components are present in the signal, and which are not.

The Short Time Fourier Transform (STFT) is essentially based on the Discrete Cosine Transform (DCT):

$$Y_m^{DCT} = c_m \sum_{n=0}^{N-1} y_n \cos\left(\frac{(2n+1)m\pi}{2N}\right), \quad (1)$$

for $m = 0, 1, ...N-1$. The scaling factor is defined as $c_m = \sqrt{1/N}$ for $m = 0$ and $c_m = \sqrt{2/N}$ for $m > 0$. Applying a smoothing window to the data modifies the DCT to the form of:

$$Y_m^{DCT} = c_m \sum_{n=0}^{\infty} y_n w_{k-nN} \cos\left(\frac{(2n+1)m\pi}{2N}\right), \quad (2)$$

with w_{k-nN} the window that covers the discrete time domain from nNT_s to $(n+1)NT_s$, with T_s the sampling period of the signal and smoothness the sequence in the interval of data points between $\left[y_{nNT_s}, \cdots, y_{(n+1)NT_s}\right)$.

Creating a spectrogram using the STFT is a digital process. The sampled data, in the time domain, is divided into windows w_{k-nN}, which usually overlap, and Fourier transformed to calculate the magnitude of the frequency spectrum for each window. Each window then corresponds to a vertical line in the image; a measurement of magnitude versus frequency for a specific moment in time. The spectrums or time plots are then 'put side by side' to form the (Jet-colored) image or a three-dimensional surface. The spectrogram returns the Power Spectral Density (PSD) of each window in dB. In this study, an overlap between windows was 50%, with Kaiser windows of length 512 samples and $\beta = 5$.

The spectrogram is an interesting tool for non-stationary signals, such as those encountered in intra-patient variability. A spectrogram is a plot of these frequency components against time; in other words, it shows how the spectral density of a signal varies in time. For plotting the spectrogram results, a 'Jet' color-map was used in this study: the more reddish the patch, the greater the magnitude of a certain frequency component over a certain period of time and the less the amplitude, the more deep the blue color in that period of time. In this study, linear axes were used to represent time and frequency. It is expected that when an artefact occurs, the energy of EEG spectrogram in that time period increases.

IV. MODELING BLOOD FLOWS

To understand the physiological effect of a stroke is necessary to provide models for blood flow - which could be correlated later on with Magnetic Resonance Imaging (MRI) data or similar tools for evaluating blood flow in brain areas affected by stroke and/or aneurysm [13]. Classical constitutive relationship for shear stress in terms of the velocity gradient can be expressed as [14]:

$$\tau = \mu \frac{du}{dy} \quad (3)$$

with τ the viscous shear stress, μ (kg/m s) the dynamic viscosity, u the flow velocity (m/s) and y (-) the radial direction in normalized form, i.e. $y = r/R$ with R (m) the radius of the pipeline and r (m) the radial coordinate. This relation no longer holds for non-Newtonian fluids as blood, detergent, gel, plasma etc.

Our previous work on fictionalizing compartmental models for drug concentration gradients in blood and tissue has indicated that each gradient can be expressed in terms of its kernel and integral form of mass transfer [15], [16]. Consider the pipeline with our fluid divided in compartments of equal infinitesimal distance. The gradient is given by:

$$u(1) - u(0) = k \int_0^1 M(\tau) d\tau \quad (4)$$

where the M denotes mass or molar amounts of material in the respective compartment, k (1/s) are rate constants. Each of the mass transfer integral includes a kernel, i.e.:

$$u(1) - u(0) = k \int_0^1 K \cdot \tilde{M}(\tau) d\tau \quad (5)$$

In the classic theory case, the kernel is simply equal to one. By choosing the kernel in an appropriate form of power-law, we can then use Riemann-Liouville fractional integrals or others. This power-law kernel has been formerly introduced in earlier studies of non-Newtonian materials and fluids [17], [18], [19]. For instance, using the kernel:

$$K(t, \tau) = \frac{(t-\tau)^{\alpha-1}}{\Gamma(\alpha)} \quad (6)$$

with $0 < \alpha < 1$, we have for $\alpha = 1$ the classical case since $K = 1$. Keeping in mind the Riemann-Liouville fractional integral is:

$${}_0D_t^{-\alpha} M(t) = \int_0^1 \frac{(t-\tau)^{\alpha-1}}{\Gamma(\alpha)} \tilde{M}(\tau) d\tau \quad (7)$$

with D standing for an integral when the order is negative and for a derivative when the order is positive. Finally, we can write (5) as:

$$u(1) - u(0) = k_0 D_t^{-\alpha} M(t) \quad (8)$$

The zero initial values are common in compartmental models, but if it is not zero, we can use the Caputo derivative, in the form:

$${}_0D_t^{1-\alpha} M(t) = {}_0^C D_t^{1-\alpha} M(t) + \frac{M(0) t^{\alpha-1}}{\Gamma(\alpha)} \quad (9)$$

where the superscript C on the left denotes a Caputo fractional derivative. Note the units of the rate constant are no longer $time^{-1}$ but $time^{-\alpha}$. This implies existence of

a memory in the tissue, i.e. the memory of the viscoelastic material perceived as deformation and other related non-zero initial conditions.

In [20] has been proposed a model to describe time-dependent flow in non-Newtonian fluids:

$$\tau(t) = \tau_0 + a \cdot \lambda_\beta \frac{d^{\beta-1}\dot{\epsilon}}{dt^{\beta-1}} \tag{10}$$

with $0 \leq \beta \leq 1$, a and λ are material constants, and ϵ (m) denotes strain. This is a generalization of (3) following the fictionalization rationale. This has been used (in various forms) to model Maxwell elements in mechanical models of viscoelasticity [17], [18]. Further on, these mechanical models are then the basis for electrical model analogous [19], [21].

To address the non-locality problem of properties in non-Newtonian fluids, one may use (10), for $0 < \alpha = \beta - 1 < 2$. The physical basis for this non-uniform velocity gradient can be the non-uniformity of fluid particles (e.g. mixtures of solid and liquid particles), molecular interaction, biological and chemical effects. Using the fractional derivative definition from [20],

$$\frac{d^\alpha u(y)}{dy^\alpha} = \frac{1}{\Gamma(n-\alpha)} \int_0^y \frac{u^n \tau}{(y-\tau)^{\alpha-n+1}} d\tau \tag{11}$$

with $n-1 < \alpha \leq n$, and n the smallest integer greater than the order α, the relationship between velocity gradient and viscous shear stress is given by:

$$\tau = \begin{Bmatrix} \tau_0 + \mu I^{1-\alpha} \frac{du}{dy}, 0 < \alpha < 1 \\ \tau_0 + \mu \frac{du}{dy}, \alpha = 1 \\ \tau_0 + \mu I^{2-\alpha} \frac{d}{dy}\frac{du}{dy}, 1 < \alpha < 2 \end{Bmatrix} \tag{12}$$

where $I^{1-\alpha}$ and $I^{2-\alpha}$ represent the fractional integral

$$I^\gamma f(y) = \frac{1}{\Gamma(\gamma)} \int_0^y (y-\tau)^{\gamma-1} f(\tau) d\tau, \gamma > 0 \tag{13}$$

This solution for flow plug profiles can be lumped into a parametric model preserving the non-integer order. For this, geometry of the brain surface and volume is used, as proposed in [22].

V. DISTRIBUTED PARAMETER TO LADDER NETWORK MODEL

By analogy to electrical networks, one can consider voltage as equivalent for pressure P and current as equivalent for flow Q. Electrical resistances R represent molecular friction resistance, electrical capacitors C represent volume compliance in a relative local geometry, electrical inductors L represent inertia of the moving molecular mass or object and electrical conductances G represent the viscous head losses (as the brain matter has viscoelastic properties).

Based on our previous works on electrical analogues of biological systems with morphology and geometry [23], one obtains a generalization via recurrence the form of the total admittance with $m = N$ cells, for $N \to \infty$:

$$Y_N(s) = \cfrac{1/Zl_1(s)}{1 + \cfrac{Zt_1(s)/Zl_1(s)}{1 + \cfrac{Zt_1(s)/Zl_2(s)}{1 + \cfrac{Zt_2(s)/Zl_2(s)}{\cdots \cfrac{\cdots}{1 + \cfrac{Zt_{N-1}(s)/Zl_N(s)}{1 + Zt_N(s)/Zl_N(s)}}}}}} \tag{14}$$

which is, in fact, a continued fraction expansion. A full analysis of various type of ladders under various conditions and denoting different applications have been introduced and discussed in [24]. It follows that generically, such systems converge as cell number goes in the limit $N \to \infty$, to a lumped parameter impedance model of the form:

$$Z_N(s) = \frac{1}{Y_N(s)} \cong \frac{K(\lambda, \chi) \cdot A}{(R_{e1} C_{e1} s)^n} \tag{15}$$

with the fractional order n given by:

$$n = \frac{\log(\lambda)}{\log(\lambda) + \log(\chi)} \tag{16}$$

with λ, χ recurrent values for the dominant properties (e.g. resistance and capacitance) along the ladder network and K a generic gain value dependent on the intrinsic relations between the cells (i.e. recurrent or equal), A being a parameter dependent on the cell elements in the transversal and longitudinal impedance values. Hence, relation (15) shows the link between the ladder network and the appearance of a fractional order term in the form of total input impedance. In the frequency domain, the fractional order will lead to a constant-phase behavior, i.e. a phase-locking in the frequency range given by the convergence conditions [22], [23], [24]. Depending on the number of cells in the ladder (N), the constant-phase behavior will emerge over a wider range of frequencies. This result is applicable to any kind of ladder network (airways, arteries etc). However, the fractional order value and coefficients will change according to the properties (morphology, geometry) of the system.

Notice the lumped impedance models are linear parameter-varying (LPV) type models, since their values are an approximated capture of the local properties. As the features of the blood flow in the brain-environment are changing, their parameter values will also change and identification can be recursively performed to mark the current position and time instant. In this way, both EEG signal data and image based MRI can provide insight into blood flow in brain based on time and location. The methodology enables technology advance for a patient monitoring system in a wearable context or in hospital-based monitoring periods.

An analytical model of neuronal pathway has been proposed in [22], based on distributed parameter system approach and lumped fractional order model parameters. In short, we generalize the differential and integral operators into one fundamental operator $D^\alpha(t)$ (with non-integer order of the operation) [22], [23], [25], [26]. As mentioned above, this is a fundamental operator, a generalization of integral

and differential operators (differ-integration operator), and can be introduced as Laplace operator in the form:

$$LD^{\alpha}(t)f(t) = s^{\alpha}F(s) \tag{17}$$

where $F(s) = Lf(t)$ and s the Laplace complex variable. The Fourier transform is obtained by replacing $s \longrightarrow j\omega$ and the equivalent frequency-domain expression is given by:

$$s^{\alpha} \longrightarrow (j\omega)^{\alpha} = \omega^{\alpha}(\cos \pi/2 + j \sin \pi/2) \tag{18}$$

These tools have been employed to develop the physiological pathway and electrical analogue given in Figure 1. The cumulative terms in the complete nociceptor model is then given by:

$$Z_{FOIM}(s) = \frac{T}{s^{\alpha_1}} + D + \frac{M}{s^{\alpha_2}} + Ps^{\alpha_3} \tag{19}$$

where $0 < \alpha_{1,2,3} < 1$ and T denotes transmission, D denotes transduction, M denotes modulation and P denotes perception, all real numbers.

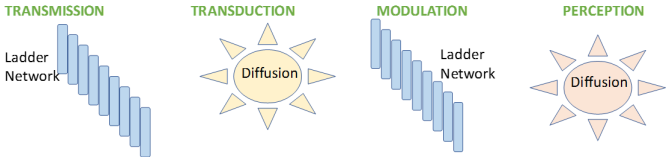

Fig. 1. Summarizing the neuronal pathway in stroke incidence.

Iterative nonlinear least squares identification was applied to the EEG signal to identify the model parameters.

VI. Results and Discussion

This section presents some of the initial results for the monitoring of EEG signal and afferent model in post-operatory patients. Figure 2 depicts a sequence with lack of events in the EEG signal represented as time based and wavelet spectrogram based graphics. The color jet indicates projections of energy of the signal from lower (blue-green) to higher (orange-red) values.

Figure 3 depicts a sequence with an event in the EEG signal represented as time based and wavelet spectrogram based graphics. The color jet indicates higher values than in the nominal case.

The identification of the model from (19) delivered an initial set of parameters for the two cases of nominal and eventful cases of EEG dynamics. Only two parameters were significantly changing with the data, i.e. the transmission and perception terms. The results are given in figures 4 and 5, respectively.

Although these are preliminary first hand results, they suggest that the proposed methodology and tools may be suitable for the objective of stroke detection and later on prevention (by detecting pre-stroke events in the EEG signal). The proposed model structure seems over-parameterized, but investigation into other events related to stroke visible in EEG signal may require the extra parameters - this study is ongoing.

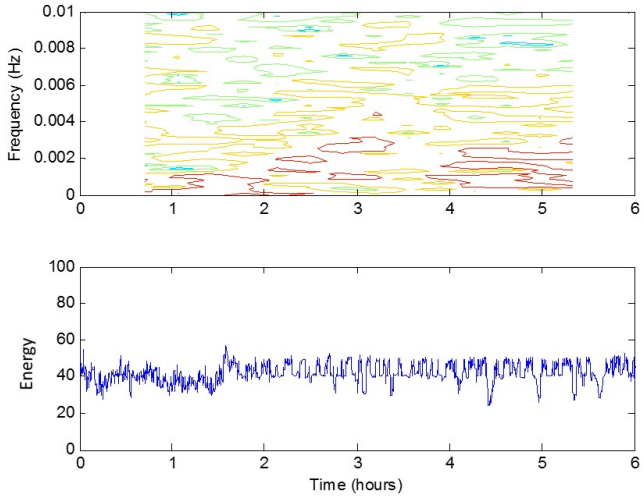

Fig. 2. Spectrogram and processed EEG signal for nominal neuronal dynamics.

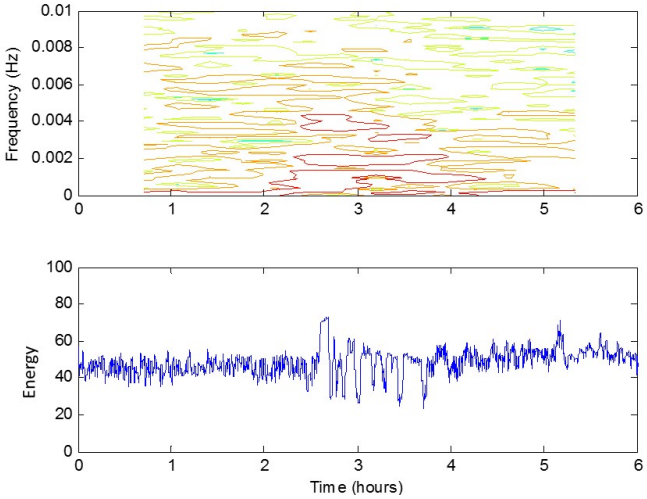

Fig. 3. Spectrogram and processed EEG signal for event-related neuronal dynamics.

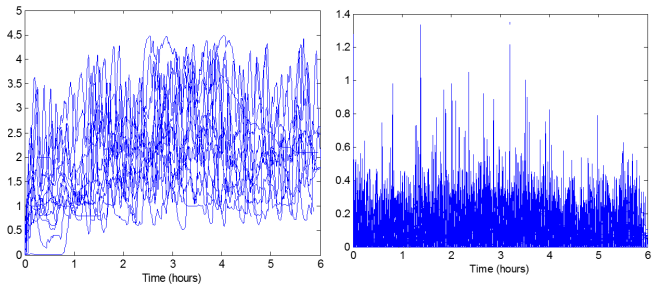

Fig. 4. Identified model parameters values for the transmission term T (left) and α_1 (right).

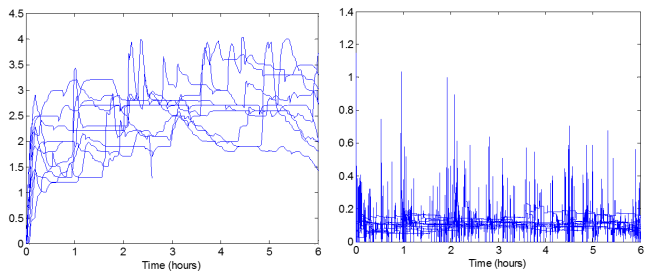

Fig. 5. Identified model parameters values for the perception term P (left) and α_3 (right).

VII. CONCLUSIONS

This paper introduced emerging tools from fractional calculus and afferent models for EEG signal processing and identification. We provided a physiological background as to the use of fractional order models and motivated the appearance of the fractional order terms from electrical analogy to neuronal dynamic pathways. The preliminary results indicate redundancy in model parameters, but further analysis of this study is ongoing.

ACKNOWLEDGMENT

This work was partly supported by a grant of the Flanders Research Centre, nr. G026514N.

REFERENCES

[1] A. Ringer and L. Jimenez. Unruptured brain aneurysm, 2018. [Online]. Available: https://www.mayfieldclinic.com/pe-aneurun.htm.

[2] J. Greving, M. Wermer, R. Brown, A. Morita, S. Juvela, M. Yanekura, T. Ishibashi, J. Torner, T. Nakayama, G. Rinkel, and A. Algra. Development of the phases score for prediction of risk of rupture of intracranial aneurysms: a pooled analysis of six prospective cohort studies. *Lancet Neurol.*, 13(1):59–66, 2014.

[3] C. Vladescu, S.G. Scintee, V. Olsavszky, C. Hernandez-Quevedo, and A. Sagan. Romania: Health system review. *Health systems in transition*, 18(4), 2016.

[4] GHDx. Global health data exchange. global burden of disease study 2015, 2015. [Online]. Available: ghdx.healthdata.org/gbd-2015.

[5] S. Szatmári, I. Pascu, L. Mihálka, S.V. Mulesa, I. Fekete, B. Fülesdi, L. Csiba, G. Zselyuk, J. Szász, J. Gebefügi, S. Nicolescu, D. Văsieşiu, V.I. Smolanka, and D. Bereczki. The mures-uzhgorod-debrecen study: a comparison of hospital stroke services in central-eastern europe. *Eur J Neurol*, 9(3):293–296, 2002.

[6] E.W. Wilkins, L. Wilson K. Wickramasinghe, P. Bhatnagar, J. Leal, R. Luengo-Fernandez, R. Burns, M. Rayner, and N. Townsend. European cardiovascular disease statistics 2017, european heart network, 2017. [Online]. Available: www.ehnheart.org.

[7] OECD. Organisation for economic co-operation and development (oecd), health care quality indicators: acute care, 2014. [Online]. Available: https://stats.oecd.org/.

[8] G.Y. Wong, D.O. Warner, D.R. Schroeder, K.P. Offord, M.A. Warnerand P.M. Maxson, and J.P. Whisnant. Risk of surgery and anesthesia for ischemic stroke. *Anesthesiology*, 92(2):425–432, 2000.

[9] R. Magin, B. Vinagre, and I. Podlubny. Can cybernetics and fractional calculus be partners? searching new ways to solve complex problems. *IEEE Systems, Man and Cybernetics Magazine*, 4(3):23–28, 2018.

[10] M. Neckebroek, C.M. Ionescu, K. van Amsterdam, T. De Smet, P. Debaets, J. Decruyenaere, R. De Keyser, and M. Struys. A comparison of propofol-to-bis post-operative intensive care sedation by means of target controlled infusion, bayesian-based and predictive control methods. a feasibility study, under review. *J. Clinical Monitoring and Practice*, 2018.

[11] Z.B. Zhou, L. Meng, A. Gelb, R. Lee, and W.Q. Huang. Cerebral ischemia during surgery: an overview. *J Biomedical Research*, 30(2):83–87, 2016.

[12] R. Pintelon and J. Schoukens. *System Identification: a frequency domain approach*. Wiley-IEEE Press, 2001.

[13] C.M. Ionescu. A memory-based model for blood viscozity. *Commun Nonlinear Sci Numer Simul*, 45:29–34, 2017.

[14] L.G. Leal. Diffusion and related transport properties in brain tissue. *J Nonnewton Fluid Mech*, 5:33–78, 1979.

[15] A. Dokoumetzidis, R. Magin, and P. Macheras. Fractional kinetics in multi-compartmental systems. *J Pharmacokinet Pharmacodyn*, 37:507–524, 2010.

[16] D. Copot, R. Magin, R. De Keyser, and C.M. Ionescu. Data-driven modelling of drug tissue trapping using anomalous kinetics. *Chaos Solitons Fractals*, 102:441–446, 2017.

[17] H. Schiessel and A. Blumen. Mesoscopic pictures of the sol-gel transition: ladder models and fractal networks. *Mectromolecules*, 28:4013–4019, 1995.

[18] J.F. Kelly. Fractal ladder models and power law wave equations. *J of the Acoustical Soc of America*, 126(4:2072–2081, 2009.

[19] G. Ala, M. Di Paola, E. Francomano, Y. Li, and F. Pinnola. Electrical analogous in viscoelasticity. *Commun Nonlinear Sci Numer Simulat*, 19:2513–2527, 2014.

[20] D. Yin, W. Zhang, C. Cheng, and L. Yi. Fractional time-dependent bingham model for muddy clay. *J. Non-Newtonian Fluid Mech*, 187:32–35, 2012.

[21] C.M. Ionescu, J.A. Tenreiro Machado, and R. De Keyser. Modeling of the lung impedance using a fractional order ladder network with constant phase elements. *IEEE Trans Biomed Eng*, 5(1):83–89, 2011.

[22] C.M. Ionescu. Phase constancy in a ladder model of neural dynamics. *IEEE Trans Syst Man Cyb*, 42(6):1543–1551, 2012.

[23] C.M. Ionescu, A. Lopes, D. Copot, JA Tenreiro Machado, and JHT Bates. The role of fractional calculus in modelling biological phenomena: a review. *Commun Nonlinear Sci Numer Simul*, 51:141–159, 2017.

[24] A. Oustaloup. *Diversity and non-integer differentiation for system dynamics*. John Wiley Sons, Inc., 2014.

[25] C.M. Ionescu and J.F. Kelly. Fractional calculus for respiratory mechanics: power law impedance, viscoelasticity and tissue heterogeneity. *Chaos Solitons Fractals*, 102:433–440, 2017.

[26] C.M. Ionescu, W. Kosinski, and R. De Keyser. Viscoelasticity and fractal structure in a model of human lungs. *Arch. Mech.*, 62(1):21–48, 2010.